CFD Analysis of Decay Heat Removal Scenarios of the Lead cooled ELSY reactor

Michael Böttcher

Institut für Neutronenphysik und Reaktortechnik (INR), Karlsruher Institut für Technologie, KIT

Abstract

In this paper decay heat removal scenarios of the lead cooled European reactor generation IV concept ELSY are presented. Based on a CFD model of the primary loops with all their components, an analysis of the steady state operation mode is performed and the critical issues of the concept are presented. In case of a reactor shutdown the decay heat of the core can be removed by several passive systems. It can be shown that for all scenarios taken into account the temperatures can be stabilized within an acceptable range and a safe state is achieved. One exception is demonstrated in case of heat removal by isolation condensers, where in the lower parts of the steam generators at certain conditions lead freezing occurs.

1. Introduction

The nuclear reactor concept ELSY (European Lead-cooled System), presented in Fig. 1, is characterized by its very compact, innovative design. Inside the reactor vessel 8 primary loops and all their components like steam generators (SG) and primary pumps are integrated. Furthermore, 4 decay heat dip coolers (WADHR – Water Air Decay Heat Remover), symmetrically distributed around the core, are foreseen. For the permanent cooling of the outer vessel a piping system operating with air and consisting of 8 loops is foreseen. The RVACS system (Reactor Vessel Air Cooling System), whose U-pipes are mainly located in a gap between the reactor vessel wall and a heat-resistant concrete layer, which is not shown here, collects cold air by its inlets and heats it up along its way through the U-pipe loops by radiative heat transport between the outer vessel wall and RVACS U-pipe surfaces. The hot air is removed outside the plant building by a piping system with 2 chimneys at a height of 30 m acting as outlet.

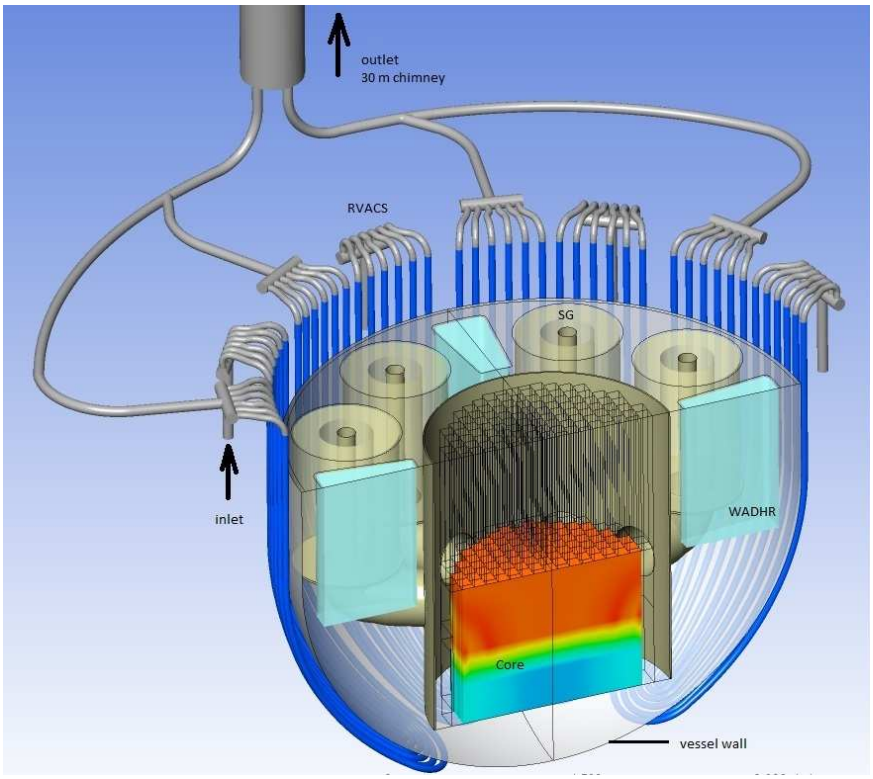

Fig. 1: Configuration of the ELSY reactor

For the primary loops lead is considered as coolant because of its chemical inertia against water and advantageous thermodynamic properties. The main disadvantages are the high solidification temperature of 327°C and the oxidation and corrosion that make the use of a purification system mandatory.

The thermal power of one unit at nominal conditions will be 1500 MW at a total mass flow rate of about 126 tons/s. As for the secondary cycle superheated water-steam is used, the thermal efficiency due to the electrical power conversion will be about 43% , which converts to an electrical power release of 600 MW. For the coolant, temperatures of 400°C at the core inlet and 480°C at the outlet are taken into account. A detailed description of the ELSY reactor is presented by Cinotti (2008).

As it is presently not possible to run a CFD model, that is able to simulate the complete primary circuit and the decay heat removal systems of a nuclear reactor in detail, several models covering only one component were developed, such as for the RVACS system by Böttcher (2009) and for the SGs by Onea et. al. (2009 and 2010). For the dip coolers (WADHR), simulations with the system code TRACE were performed by Imke (2008) in order to compute the amount of heat removed from the primary system at specific lead temperatures. These results were used as source terms for a global CFD model (by applying ANSYS CFX 11.0), that takes advantage of the reactor symmetry and covers a 90° part of the vessel including 2 of 8 primary circuits with all their components.

2. Model description

To model the ELSY reactor several individual CFD models were developed. The vessel model, which is mainly described in this paper, considers a 90° part of the vessel with all its components and consists of a hybrid mesh of about 20 million cells, see Fig. 2. The dimensions of the vessel are about 8.5 m (height) by 12 m (diameter).

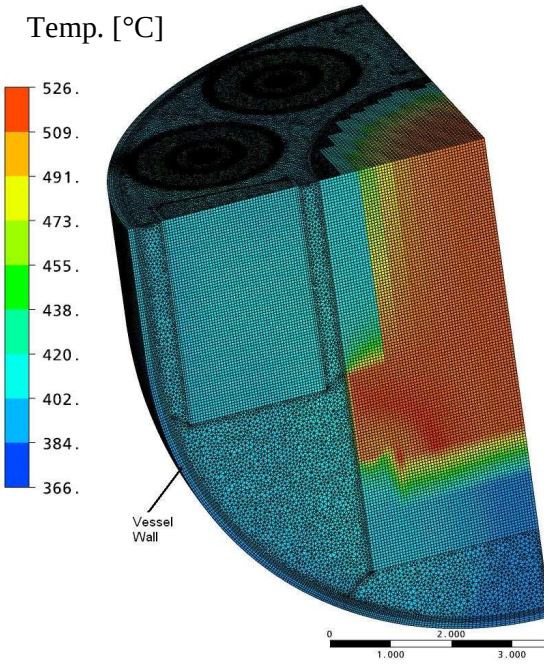

Fig. 2: The vessel model

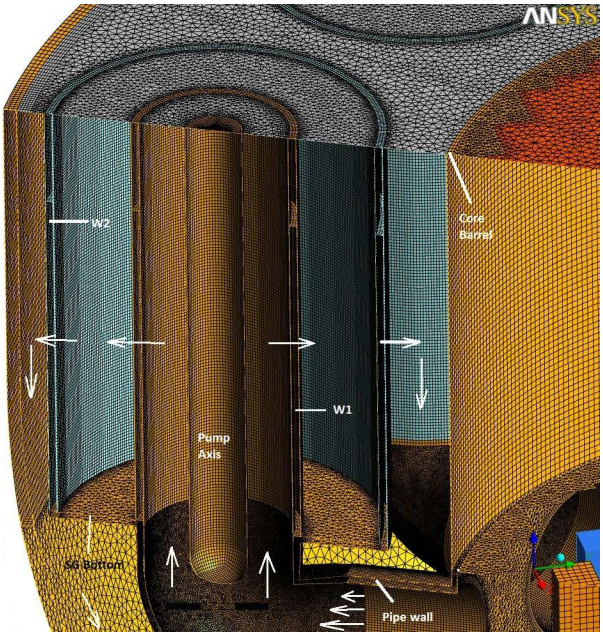

Fig. 3: Detail of the vessel model

The lengths of the cells vary between 10 mm in regions with large gradients and approximately 75 mm. Solid structures like the vessel wall, the core barrel and pipe walls are represented by the grid cells with corresponding heat conduction mechanism, see Figs. 2 and 3. Fig. 3 shows details of the

mesh inside the steam generator. The coolant enters into the lower center of the SG through radial pipes coming from the core. The lead passes through the pump impellers which are not shown here and flows upwards along the axis of the pumps. On its radial way through the SG a perforated wall (W1) has to be passed. Between W1 and the outer perforated wall W2 the heat is removed by a secondary flow cycle consisting of superheated water flow through a couple of spiral type rods. The heat sink is modeled here by a volumetric energy source term derived from a RELAP model by Barucca and Gregorini (2008). The pressure loss of W1, W2 and at the region between W1 and W2 covered with spiral type tubes is computed by using loss coefficients derived from detailed CFD models by Onea et. al. (2009), and from correlations taken from VDI Wärmeatlas (2006).

2.1 The core model

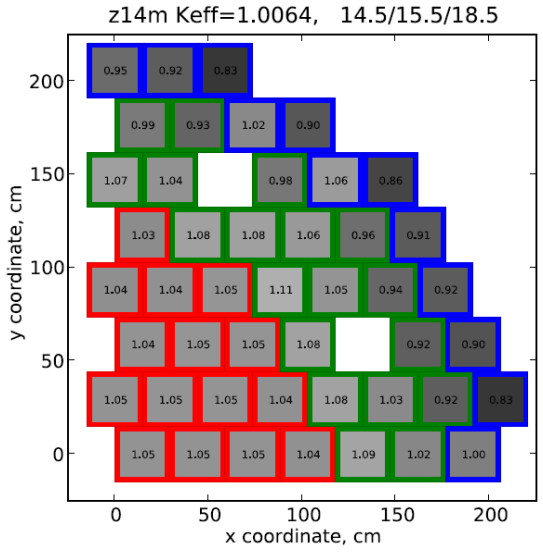

Fig. 4: Assembly power factors

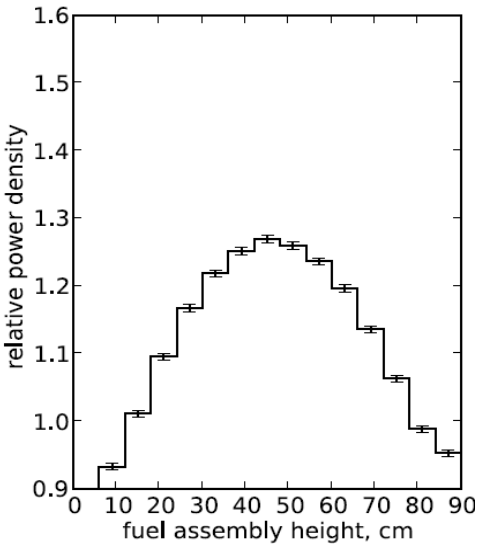

Fig. 5: Assembly axial power distribution

For the core, which is resolved on assembly basis, an open square sub-assembly design is chosen. It consists of 170 fuel assemblies with different enrichment zones with an active length of about 1 m. The active part of the core is indicated by the region with a temperature rise in Fig. 2. Each fuel assembly with a cross section of 294 x 294 mm^2 contains 428 fuel pins of mixed oxide (UO_2 and PuO_2). Fig. 4 shows the assembly power factors. The assemblies containing control rods are providing only a small amount of power and are left empty. Each cross section is meshed by 5 x 5 hexagonal cells with an axial length of 50 mm. The volumetric heat source of the core is assembly dependent with an axial power distribution given in Fig. 5. The power distribution is following the proposals of Travleev (2009).

Pressure loss coefficients based on the work of Rehme (1973) are implemented, which take into account the losses at the inlet and outlet of the core, the losses by the flow through the subchannels and of 6 spacers. At nominal conditions of 126 tons/s the pressure loss is about 0.85 bar with an average velocity in the power assemblies of 1.38 m/s. The coolant temperature in the average assembly is assumed to be 400°C at the inlet and 480°C at the outlet. The inactive upper part of the core above the radial outlets towards the SGs is considered as solid with the density, heat capacity and conductivity of liquid lead. The region between the reflector and the active part of the core is filled with dummy assemblies without power production. A bypass flow of about 3% is assumed, which is achieved by setting loss coefficients 400 times larger than for the power assemblies.

2.2 The SG model

Because of computational limitations it is not possible to resolve the perforated walls and the heat exchanging spiral pipe structures. As consequence, the frictional losses and the heat exchange have to be implemented by volumetric source terms.

The standard operation conditions of the 8 SG units are given by an average inlet temperature of 480°C and 400°C at the outlet. At standard conditions each unit has to remove 187.5 MW at a coolant flow rate of 15.75 tons/s. The formulation of the heat sink of the SGs is of main interest for the model, as it is used for establishing the temperature level of the primary loops. The heat release of the core is considered as temperature independent. The system is closed and the boundaries are treated as adiabatic except the outer vessel wall. The RVACS system is permanently removing heat, but its capacity is 3 orders of magnitude lower (at standard conditions) than the heat production by the core.

The secondary system is operating with supercritical water with a temperature of 335°C at the inlet. If the coolant on the primary side has reached this temperature, no heat is transferred anymore. A linear dependency of the heat flux based on the two fixed temperatures at inlet and outlet of the SGs is assumed. Furthermore, the influence of the local lead velocities is neglected and the heat sink is considered to be spatially constant. The volumetric source term is implemented as

$$-Q = \frac{T_{lead,in} - 335^0 C}{145^0 C} \cdot 187.5 MW / V_{SG} \qquad (1),$$

where V_{SG} is the total volume of heat exchanging region and $T_{lead,in}$ is the averaged lead temperature at the SG inlet.

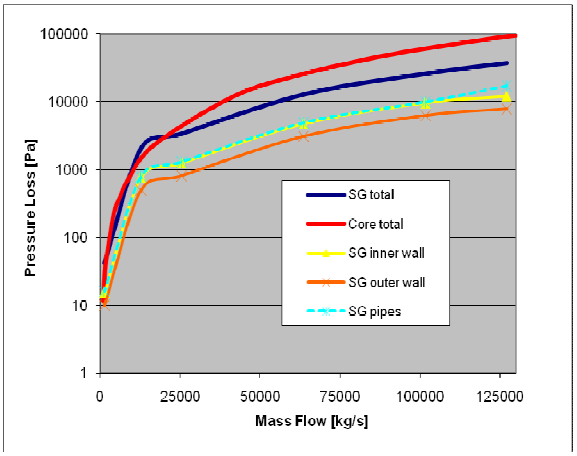

Fig. 6: Component pressure losses

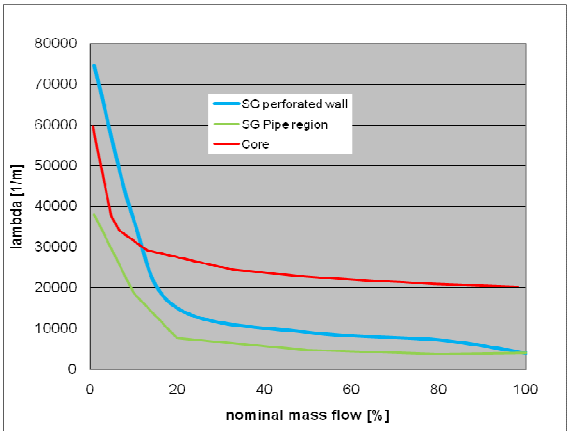

Fig. 7: Loss coefficients of components

The SGs are treated as porous media with a porosity of 0.65 for the pipe region. For the perforated wall regions a porosity of 1 is assumed. Otherwise the radial discretization by 3 cells at a radial wall thickness of 60 mm leads to convergence difficulties. Loss coefficients for the perforations and the pipe bundle region are assumed based on the results by Onea et al. (2008 and 2010). Fig. 6 presents the main pressure losses within the ELSY primary circuits. At standard conditions the pressure loss in the core is about 0.89 bar, while for the SGs about 0.3 bar is reached. The pressure loss inside the SGs is 0.103 bar for the inner perforated wall, 0.1 bar for the pipe region and 0.078 bar for the outer perforated wall. At standard conditions the pressure loss inside the core is dominant, but at free convection conditions with low flow rates the situation is changing and the influence of the losses by the SGs becomes more important. The loss coefficients of the various components are shown in Fig. 7. The implementation of the pressure losses is done as directional loss model given by

$$-\frac{\partial p}{\partial x} = \lambda \frac{u^2}{2} \rho \qquad (2),$$

where λ is the loss coefficient, u the velocity component in x direction and ρ the coolant density. For the SG perforations in radial direction loss coefficients specified by Fig. 7 are used, while for the axial and circumferential direction the loss coefficients are multiplied by a factor of 10. For the spiral tube region and for the core an isotropic loss model is applied.

For large Reynolds numbers the loss coefficients are approaching an asymptotic value, while for low Reynolds numbers they are increasing significantly. As consequence, the design of the SG due to its perforated walls becomes the limiting factor of the natural convection flow rate, if the pumps are switched off and the decay heat production of the core becomes the driving force due to density differences.

2.3 The pump model

Each of the 8 primary loops contains a pump, for which only its impeller axis is considered as non-rotating solid. The impellers are located below the bottom of each SG inside the annular channel between the pump axis and the inner perforated wall W1 (Fig. 3). They are not taken into account by the computational mesh but in terms of a volumetric momentum source. The vessel model is a closed system, so that in case of forced convection the coolant flow has to be fixed by the imposed momentum source terms of the pump impellers. A simple approach is given by a formulation of a Dirichlet type condition (see ANSYS User Manual (2009)):

$$-\frac{\partial p}{\partial x} = K(u - u_{spec}) \quad (3),$$

where K is set to a large number, e.g. 10^6 kg/m^{3}s, u is the velocity component in x-direction, which is equivalent with the pump axis, and u_{spec} is a specified velocity. For the flow volume, which is occupied by the pump impellers but left free in the CFX model, u_{spec} is set to a constant value derived from the theoretical mass flow, the density of the coolant and the local cross section area. For the components in transversal direction an equivalent formulation is used, but the specified velocity component is set to 0, so that the solution is pushed towards a parallel flow with a constant velocity u_{spec}. For more advanced models it would be possible to implement 3D velocity profiles obtained from a standalone pump model or even to resolve the pump impellers by the computational mesh and to simulate its rotations with a frozen rotor approach.

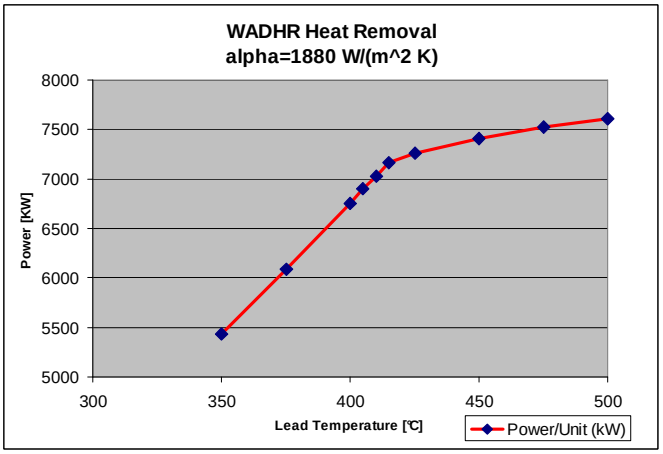

Fig. 8 : Power of a single dip cooler (TRACE model)

2.4 The dip cooler model (WADHR)

Each of the 4 dip coolers (Fig. 1) is made of a bayonet tube bundle, which can be operated in case of decay heat removal, if the isolation condenser systems (ICS), acting through the SG secondary circuits, are not available. Each WADHR loop, for which a power of 5 MW is envisaged in case of a lead temperature of 430°C, is constituted by a cooling water storage tank vertically above, so that the coolant flow is driven by gravity. Alternatively, in case of low decay heat production, an air operation mode with less power is foreseen. In the CFD vessel model the WADHR systems are considered as porous media with volumetric heat sinks, which are obtained from a TRACE model by Imke (2008) based on a heat transfer coefficient of 1880 W/(m^{2}K) and a mass flow of water of 0.023 kg/s on the secondary side, see Fig. 8. Between 0 s and 750 s after the shutdown is initiated an operation level of 16.6% (due to flow instabil-

ities on the secondary side) is assumed. Between 750 s and 1000 s the level increases with linear time dependency to 100%. For larger times full availability is assumed. The instantaneous heat exchange of the WADHR system is calculated by evaluation of the spatially averaged lead temperature inside the WADHR´s volume.

2.5 Model assumptions and boundary conditions

For the spatial discretization a 1st order donor cell method is applied in order to stabilize the simulations, especially for the transients. The time integration is performed with a 2nd order Euler-backward method with an adaptive time step management of the solver. As mentioned before a closed system is modeled, where the temperature and the mass flow are controlled by source terms. As boundary conditions a heat flux derived from RVACS CFD results is imposed on the outer vessel wall, furthermore symmetrical zero-gradient boundary conditions are used in circumferential direction. The RVACS system removes 0.83 MW at a vessel wall temperature of 400°C and 1.04 MW at 500°C with a quasi-linear dependency on the wall temperature. So for all presented cases the RVACS heat flux is evaluated by the mean vessel wall temperature and introduced as a local constant, but it needs to be pointed out that for the presented cases it is one order of magnitude lower than for the other systems.

Because the free lead surface is not taken into account, the top of the model is treated as a simplified free-slip adiabatic wall. With the exception of the vessel wall all model boundaries are considered as adiabatic. For all simulations ANSYS CFX 11.0 is used.

3. Results for the standard operation conditions

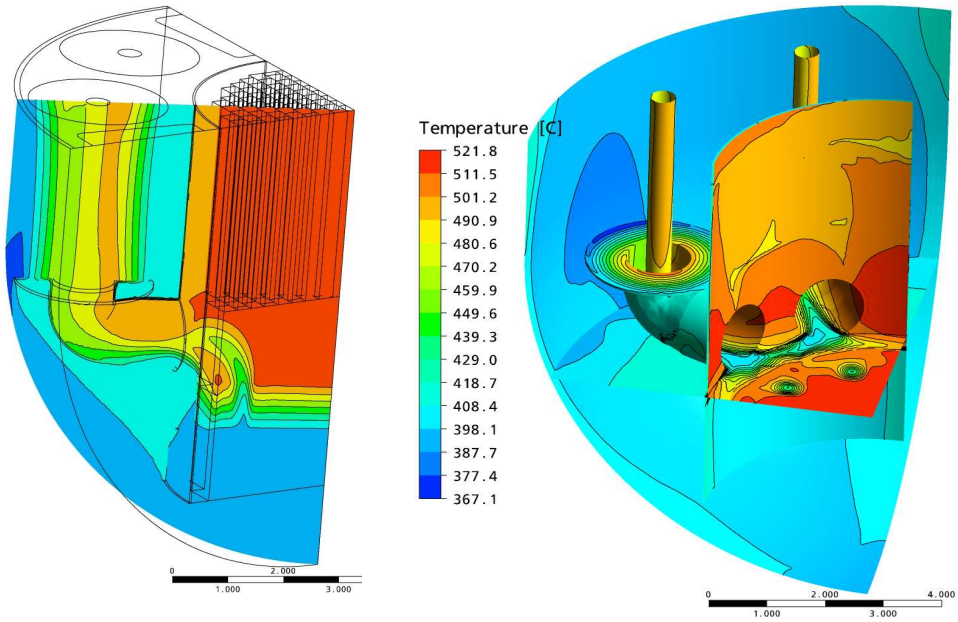

Fig. 9: Steady state temperature distribution at nominal operation conditions

As mentioned before the reactor is operating at nominal conditions, which means a thermal power production of 1500 MW and a coolant flow rate of 126 tons/s. Fig. 9 presents the temperature distribution for a case where the core reflector is considered as liquid lead and a bypass flow of 3% through the dummy assemblies is assumed. In the left part a radial cut through a control rod position is shown. An unheated jet-like structure propagates through the core just into the pipe towards the SG. Due to the high density of the liquid lead the crosswise mixture is rather small and the influence of the low power control rod assembly is – together with the unheated bypass flow- responsible for temperature differences of about 20°C at the inlet of the SG. Furthermore, strong temperature differences at the radial core pipe outlets up to 60°C are predicted, which may cause material problems due to thermal

stresses. Those temperature differences can be lowered by a core reflector of solid steel to about 30°C, but the constructive details for these parts are still an open issue.

4. Decay heat removal scenarios

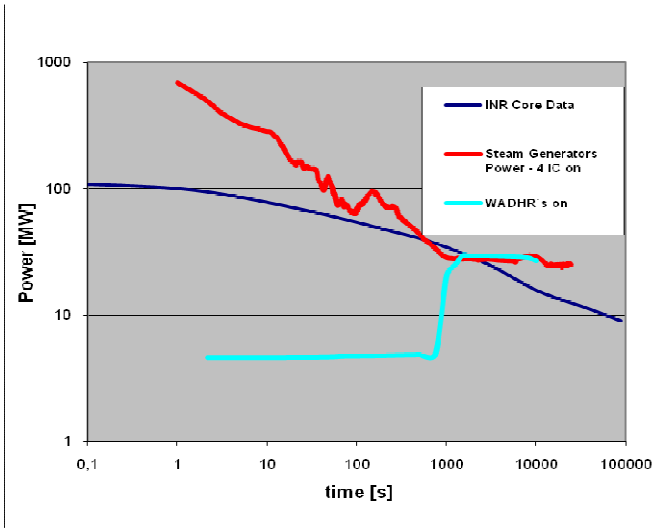

Fig. 10: Heat production and consumption

Two different cases of DHR are investigated in this paper. The first one considers the heat removal by isolation condenser systems, which are operating through the secondary circuits of the SGs, while for the other case the decay heat is removed by the WADHR systems in water operation mode. In Fig. 10 the decay heat production of the core and the heat sinks of the ICs and the WADHR systems are presented. 0.1 s after the control rods are inserted the heat production of the core has decreased very rapidly to 6% of its initial level of 1500 MW. Up to about 1000 s the isolation condensers are removing more heat than produced, while the WADHRs are starting at about 3 MW and are reaching 20 MW after 1000 s. The data for the ICs are taken from a RELAP model simulation by ANSALDO (2008) and are used as input data for the CFD simulation, as it is presently not possible to model the secondary circuit due to multiphase flow effects. The WADHR data are based on the temperature difference between lead on the primary side calculated by our CFD model and the secondary side. The volumetric averaged coolant temperature at the WADHR locations is used and the total heat consumption is derived from TRACE simulation results (Fig. 8). As mentioned before for both scenarios the heat consumption is introduced as a locally constant, volumetric sink term which is updated after each time step. Up to 10000 s are simulated by using a second order Euler-backward method with adaptive time steps. At average time steps of 6 s about 3 weeks of computational time (using 12 parallel processes) are necessary. It has to be mentioned that convergence criteria are weakened compared with the steady state calculations, because otherwise a computational time of about half a year would have been necessary. Precisely the convergence level was increased by a factor of 5 to 5e-04 for the normalized residuals, furthermore 0.01 for the global balances was applied. Compared with the standard high order discretization method the applied 1st order donor method has a higher damping and allows larger timsteps . The accuracy of the transient simulations is reduced but at least sufficient to obtain a qualitive understanding of the flow field.

5. Results of DHR studies

Fig. 11 shows the mass flow through one pump cross section for the two cases. Together with the reactor scram the pumps are shut off and because of inertia effects it is assumed, that the impellers rotation has decreased to 0 after a delay time of 5 s. The flow conditions are very rapidly changing from forced convection to buoyancy driven natural convection. The mass flow per pump decreases from initially 15.75 tons/s to values below 500 kg/s.

The design of the steam generator is important, mainly because of the wall perforations. The heat up of the coolant in the core is the driving force of a natural convection circulation due to density differences, but the core temperatures should be kept within reasonable limits. The temperature minima and maxima for the core are shown in Fig. 12. At standard conditions the average heat up of coolant in the core is about 80°C and the maximum differences (calculated by the CFD model) are about 110 °C.

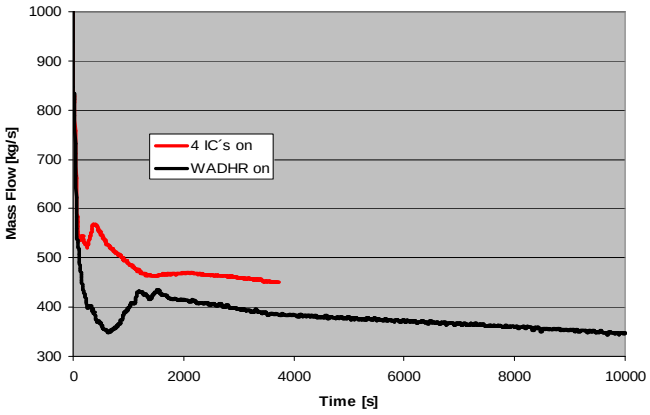

Fig. 11: Mass Flow through one pump

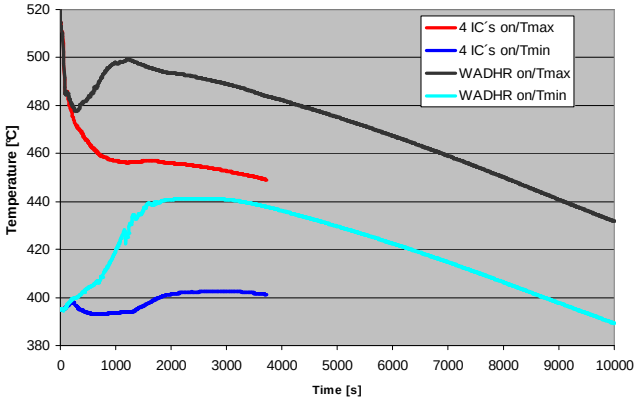

Fig. 12 : Maximum and minimum core temperatures

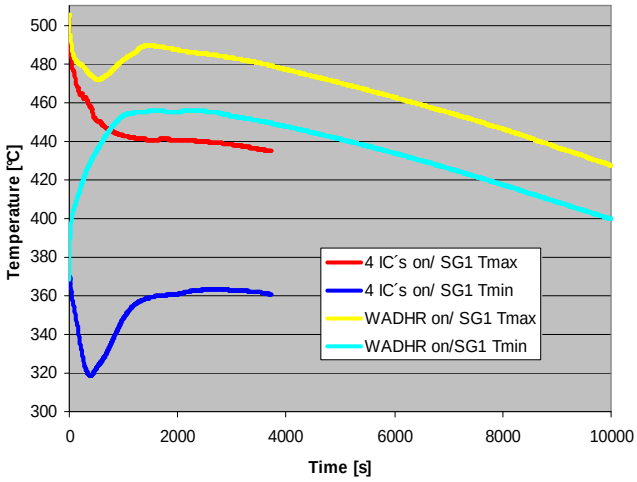

Fig. 13: Temperature minima and maxima at the SG´s

In case of natural convection and decay heat release the temperature differences become significantly smaller and are only reaching about 50°C for both scenarios.

However, there is one exception where the coolant temperatures are outside an acceptable range. Inside the steam generators the lead velocity is significantly lower close to the bottom and larger towards the top of the SG. If the heat is removed by isolation condensers, then the local heat flux mainly depends on the large temperature differences between the fluids on the primary and secondary side, while the comparatively low velocity on the primary side is of less influence. So the simulation locally predicts lead temperatures below the freezing point. 5 minutes after the ICs are started solidification at the bottom of the SGs takes place. The situation is shown in Figs. 13 and 14. Within a short time interval between 300 and 500 s the temperatures are locally below the melting point of lead (327°C), which is indicated by an iso-surface with metallic texture.

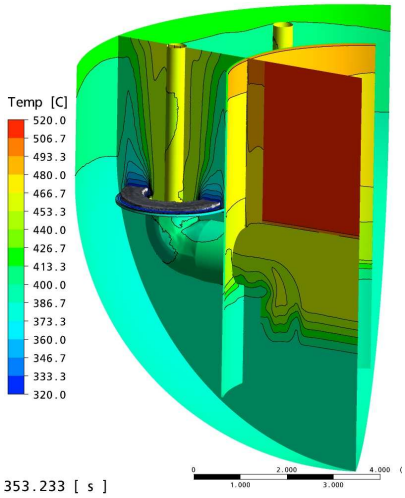

Fig. 14: IC scenario at 353 s

As consequence, a modification of the IC system and /or its operational logics seems to be necessary. The time dependent development of flow patterns for the WADHR scenario, in terms of streamlines coloured with the local temperatures, is demonstrated in Fig. 15. At 0 s the flow is in forced convection conditions which are visible by a straight global flow circulation nearly without secondary structures. The core is still operating at 100% of its nominal power, which is visible by the average heat up

of about 80°C of the lead passing through the core. At 4.9 s the flow is utmost transient dominated by the primary pumps shut off and the sudden decrease of the core power. The initial structures of the forced convection flow are still visible, but additional large scale structures similar with a stop vortex below the SG bottom level are developed now. Furthermore the flow seems to be noisier in detail, which may be due to the reduced convergence criteria of the transient calculation against the steady state solution. After 1000 s the average lead temperature has increased by more than 20°C because up to this time the decay heat of the core is larger than the removed heat of the WADHR systems. At 10000 s the average coolant temperature has decreased again because now more heat is removed as produced. It can be stated that the natural convection is stable for both scenarios and for all times the coolant temperature is well above the melting point with one exception discussed before. Also, the structural integrity of core materials is not compromised.

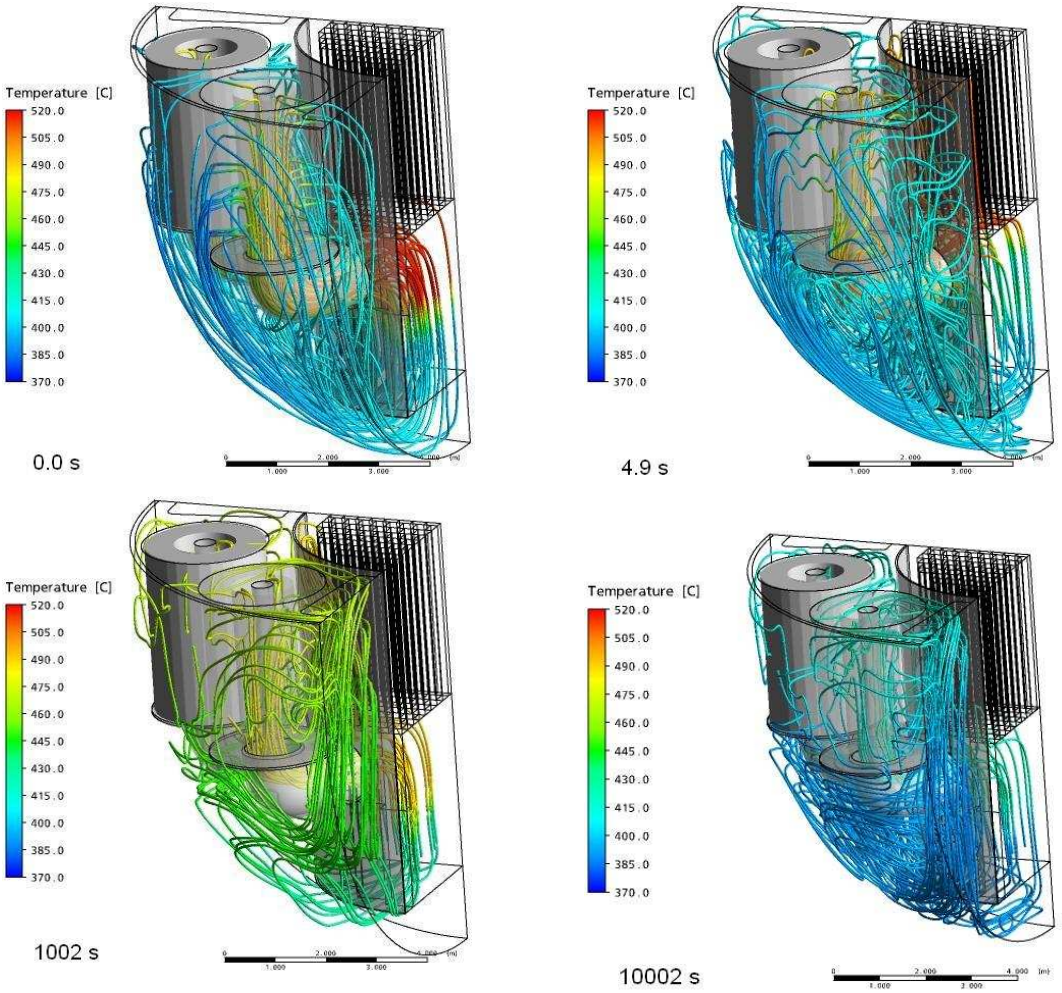

Fig. 15: Flow situation for the WADHR scenario

6. Summary and conclusions

In this paper a detailed CFD investigation of the ELSY reactor concept at nominal operation conditions and for decay heat removal scenarios is presented. It is shown that the concept is working in principle but there are some points which still have to be improved, mainly strong temperature gradients at the core outlet. In case of a reactor shutdown the passive heat removal systems are working in stable conditions and the temperatures can be controlled in an acceptable range. For the case of heat removal by isolation condenser systems a solidification of lead close to the steam generator bottom is possible. Apart from a modification of the IC systems the flow through the steam generators could be homogenized by the introduction of an axial dependent pressure loss of the perforated SG inner and

outer walls, which should be larger in the upper parts. For future Gen. IV systems the innovative compact design of ELSY provides an interesting approach because of its safety and commercial aspects.

6. References

L. Barucca, M. Gregorini, "DHR Main components Functional Sizing", *DOC/08/047*, Ansaldo Nucleare, (2008).

M. Böttcher, "CFX Analyses of the RVACS Decay Heat Removal System", *KIT/INR-09-01*, Wissenschaftliche Berichte, (2009).

L. Cinotti, "Reactor Assembly preliminary Configuration", *ELSY DOC 08 049*, Del Fungo Giera Energia, (2008).

Gnielinski et. al., *VDI-Wärmeatlas*, Springer-Verlag Berlin Heidelberg, (2006).

U.Imke, "Trace simulations of the ELSY dip coolers", private communication, (2008).

A. Onea, M. Böttcher, D. Struwe, "Analysis of the pressure loss through the heat exchanger for the primary side of the ELSY nuclear reactor", *KIT/INR-09-03*, Wissenschaftliche Berichte, (2009).

A. Onea, M. Böttcher, D. Struwe, "Detailed CFD analysis of the pressure loss on the primary side for the heat exchanger of the ELSY fast lead-cooled reactor by applying unit slice models", *ASME-ATI-UIT*, Sorrento, 16-19 May, (2010).

K.Rehme, "Pressure drop correlations for fuel element spacers", Nuclear Technology, Vol. 17, p.15-23, (1973).

A.Travleev, "ELSY core design static, dynamic and safety parameters with the open square FA; Appendix C: Preliminary Core Analysis",*FPN-P9IX-006*, ENEA,(2009).